Four Decades of Progress in Monitoring and Modeling of Processes in the Soil-Plant-Atmosphere System: Applications and Challenges

Bayesian inference of tree water relations using a Soil-Tree-Atmosphere Continuum model

J. Rings[a], T. Kamai[a], M. Kandelous[a], P. Hartsough[a], J. Simunek[b], J. A. Vrugt[c], and J.W. Hopmans[a]*

[a]*Department of Land, Air and Water Resources, University of California, Davis, CA, USA*
[b]*Department of Environmental Sciences, University of California, Riverside, CA, USA*
[c]*Department of Civil and Environmental Engineering, University of California, Irvine, CA, USA*

Abstract

To better understand root-soil water interactions, a mature white fir (Abies concolor) and the surrounding root zone were continuously monitored (sap flow, canopy stem water potential, soil moisture, and temperature), to characterize tree hydrodynamics. We present a hydrodynamic flow model, simulating unsaturated flow in the soil and tree with stress functions controlling spatially distributed root water uptake and canopy transpiration. Using the van Genuchten functions, we parameterize the effective retention and unsaturated hydraulic conductivity functions of the tree sapwood and soil, soil and canopy stress functions, and radial root zone distribution. To parameterize the in-situ tree water relationships, we combine a numerical model with observational data in an optimization framework, minimizing residuals between simulated and measured observational data of soil and tree canopy. Using the MCMC method, the HYDRUS model is run in an iterative process that adjusts parameters until residuals are minimized. Using these optimized parameters, the HYDRUS model simulates diurnal tree water potential and sap flow as a function of tree height, in addition to spatially distributed changes in soil water storage and soil water potential.

Keywords: hydraulic properties; tree ET; numerical modeling; parameter optimization

1. Introduction

Trees and forests play a key role in controlling the water and energy balance at the land-air surface. By way of biophysical principles, soil water is taken up by the roots and moves through the water-conducting

---

* Corresponding author. Tel.: 530-752-3060.
E-mail address: jwhopmans@ucdavis.edu.

vessels or xylem along a water potential gradient into the canopy, where it transpires into the atmosphere through leaf stomata. The changing soil water content affects both hydrological and tree responses, by way of regulating stream flow transpiration rates, and ecosystem functions.

Numerical water flow models allow simulating the relevant soil hydrological processes in their most basic form, such as water infiltration, soil water redistribution and deep percolation, as well as water uptake by roots and the effects of soil water stress on tree transpiration. Early attempts to model tree water flow were often based on the electrical circuit analog [1], with resistance-capacitance (RC) models to characterize xyleme resistance to water flow and water storage, and allowing for a time lag between sap flux density and transpiration rate [2,3]. Subsequent models of varying complexity were introduced using the RC approach [4,5,6], however, problems arise to fully describe the measured spatio-temporal variations in tree hydraulic conductance and water storage, as controlled by tree water potential, with the changing xylem saturation caused by partial cavitation of the tree conducting vessels [7].

Though models were improved, for example by considering hydraulic capacitance being a function of water potential, more recent studies have abandoned the RC approach and instead embraced the physically-based nonlinear modeling framework [7,8,9,10,11,12], as typically applied for unsaturated water flow modeling [13,14]. These numerical flow models discretize the modeled domain into small elements and use finite-difference or finite-element methods to solve the flow equations. However, few models use the integrated soil-tree continuum approach, coupling the soil with the tree domain, simulating the soil, roots and tree trunk as a continuum, in which water flow is driven by water potential gradients along the coupled Soil-Tree-Atmosphere-Continuum or STAC [12,15] with spatially-distributed root water uptake and canopy transpiration sink terms.

By way of the coupled hydrodynamics flow model at the tree scale, water flow through the tree root system and stem is driven by the evaporative demand and soil-available water, leading to a gradient in xylem water potential along the STAC. Water flow through the coupled system is described using the Richards' type unsaturated flow equation [16], with both the soil and tree conducting domains modeled as a porous medium, defined by nonlinear soil and tree water relationships. As part of the STAC, the coupled model computes the spatial-temporal changes inthe xylem water potential, xylem water content and xylem water flux or sapflow, along the tree trunk. Potential tree transpiration is reduced by a water potential dependent reduction function to determine actual tree transpiration. By defining a tree trunk water capacity term, the model is able to simulate the dynamic behavior of tree hydraulics, including the control of tree water storage and xylem conductivity on tree transpiration.

Bittner et al. [15] were among the first to apply the coupled soil-tree porous media model to simulate tree hydrodynamics by solving the mass-conserving PDE or Richards model, that solves for the spatial-temporal dynamics of the tree hydraulic system, from which tree transpiration can be determined from simulated sap flux densities as computed from xylem axial conductances and water potential gradients along the tree stem and canopy, and including a sink term to represent spatially-distributed canopy transpiration. Tyree [5] already showed the importance of including tree hydraulic architecture and geometry with corresponding hydraulic conductance and stem water capacitance on matching measured tree water dynamics, controlling tree response to changing soil water conditions, with tree trunk water storage and changing unsaturated conductivity caused by cavitation of the water-conducting vessels in the sap wood [7]. Bitter et al. [17] demonstrated that differences in stomatal closure and drought tolerance between tree species is caused by differentiation in tree xylem properties between species.

Soil tree hydraulic parameters can be measured in the laboratory, however these measurements are difficult and mostly destructive. For the purpose to achieve representative tree water relationships their parameters must be calibrated by comparison of simulated with observational data. Alternatively, as has been done for soils [18,19], effective hydraulic parameters can be obtained through an optimization framework, whereby residuals between measured and model-simulated variables are minimized. The

main objective of our paper is to estimate the tree hydraulic relationships and their control on tree water stress and transpiration, using a global parameter optimization technique.

2. Site description and measurements

Measurements were conducted in and around a White Fir (*Abies concolor*) in a 99 ha subcatchment (P301) of the King's River Experimental Watershed (KREW), located in the rain-snow transition zone of the southern Sierra Nevada mountain range in California at an elevation of 2018m. This study is part of the Southern Sierra Critical Zone Observatory (CZO), established to improve understanding of surface and subsurface processes along a gradient of elevation, energy, water, and soil [20,21]. The White Fir (CZT-1) is located along a ridge in a relatively open area of the forest at an elevation of 2018 m (Bales et al., 2011b), near a meteorological station. The mature tree is about 30 m high, with a trunk diameter of 0.55 m.

Undisturbed soil samples were collected to a depth of 2.5m for soil analysis. The top 1 m soil was a loamy sand to sandy loam with a range of sand content from 70-84 %, with sand content increasing from 84-90 % below the 1 m soil depth. Dry bulk density values ranged from about 1.0 g cm^{-3} (15 cm sampling depth) to about 1.4 g cm^{-3} (60 and 90 cm sampling depth) and increasing to near 1.5 g cm^{-3} at the 2.5 m depth. Corresponding measurements of saturated hydraulic conductivity using the constant head method [22] showed values between 5-10 cm/hr in the top 1 m, decreasing to around 1 cm/hr in the 1-2.5 m depth interval. Soil hydraulic parameters for soil samples of the top 1 m were obtained using the modified multistep outflow method as presented by Nasta et al. [23]. Excavations further down below 2.5 m indicated the presence of weathered bedrock that changes with depth to moderately dense saprolite and consolidated saprock and hard bedrock below 5m.

Data used in the presented study include soil moisture, tree sap flux and stem water potential measurements, with the meterorological data of the flux tower providing the necessary information for potential tree evapotranspiration. Data were selected for an 18-day rainless period in summer of 2009, starting July 15. Echo- 5TE soil moisture sensors were installed at depths of 0.15 m, 0.30 m, 0.60 m and 0.90 m in each of 6 locations within a 5 m radius from the tree trunk. The sensors were calibrated in the laboratory [24], from which it was determined that their accuracy is around 3% for a range of soils. Using all water content measurements, average total soil water storage (m^3) was computed during the 18-day measurement period every half hour. Three sapflow sensors (TransfloNZ, Palmerston North, NZ) were installed into the sapwood at a trunk height of 2.5m. Using the compensation heat pulse technique (Green and Clothier 1988), average sap flux flow (L/d) was estimated at 30-minute time intervals. All soil moisture and sapflow data were stored by a data logger. Stem water potential measurements were taken [25] from needle stems of various lower tree branches, at about 6 m from the ground. Seven measurements were taken during 24 hours on July 21-22, 2009.

3. Soil-Tree-Atmosphere-Continuum Model

By way of numerical flow modeling, the overall goal is to identify the physical processes and hydrological properties that control spatial and temporal changes in water flow of the coupled soil-tree-atmosphere domain. The requirements for this model are to (a) simulate time series of tree sap flow and stem water potential, soil water content and matric potential, and (b) to couple collected data with numerical flow simulations, allowing estimation of tree water relationships (water retention and unsaturated hydraulic conductivity functions). The STAC model is driven by spatially distributed potential evaporation in the canopy and includes reduction functions of potential evapotranspiration (ET) and root water uptake as determined by leaf and soil water potential, respectively. In order to estimate

deep soil water contributions to tree ET, the soil domain was extended to 5 m depth. The following model was developed for the main purpose to characterize and identify the main physical processes that control tree response to limiting soil water availability conditions, requiring coupling of soil with tree domains using the unifying concept of water potential that drives water through the STAC.

3.1. Unifying Equations

Across the soil-tree domain, unsaturated water flow is described by the Richards equation [16], as presented here in its axisymmetrical, two-dimensional, isotropic form

$$\frac{\partial \theta}{\partial t} = \frac{1}{r}\frac{\partial}{\partial r}\left(rk_r\frac{\partial h}{\partial r}\right) + \frac{\partial}{\partial z}\left(k_z\frac{\partial h}{\partial z}\right) - \frac{\partial k_z}{\partial z} - W(h,r,z) \tag{1}$$

where θ is the volumetric soil water content (m^3 m^{-3}), k defines the unsaturated hydraulic conductivity function (md^{-1}), h is the soil water pressure head (m), r is the lateral coordinate, z is the vertical coordinate (positive downwards), t is time (T) and $W(h,r,z)$ defines a sink/source term (m^3 m^{-3} d^{-1}) that quantifies either spatially distributed root water uptake (soil, W_{Soil}) or canopy transpiration (tree, W_{Tree}). Both k and W are functions of θ and/or h. The subscripts r and z allows for the possibility to include soil anisotropy, i.e., to simulate water flow with the unsaturated hydraulic conductivity function being different for the r- and z-direction.

For solution of Eq. [1], the water retention and unsaturated hydraulic conductivity functions must be defined for both the soil and tree conducting matrix, with the retention function characterizing water storage capacity. We define these functions using the relationships of [27,28], using the degree of effective saturation, S_{eff}, or

$$Seff = \frac{\theta - \theta_r}{\theta_s - \theta_r} = (1 + |\alpha h|^n)^{-m} \tag{2}$$

and

$$k(h) = k_s\sqrt{S_{eff}}\left(1 - (1 - S_{eff}^{\frac{1}{m}})^m\right)^2 \tag{3}$$

where θ_s denotes the saturated water content at $h = 0$ (m^3 m^{-3}), θ_r is the residual water content (m^3 m^{-3}), α and n ($m=1-1/n$) are shape parameters, and k_s is defined as the saturated conductivity at $\theta = \theta_s$ (m d^{-1}).

3.2. Domain Definition, Boundary and Initial Conditions

We use the finite element HYDRUS software [14], to solve the Richards Eq. (1) in a discretized system of linear equations, for water potential, volumetric water content and water flux density across the coupled soil-tree domain and assuming axial symmetry around the tree trunk. Both the soil and tree trunk are modelled as axial-symmetrical, represented by a rectangular domain (Fig. 1). The simulated soil domain extends to 5 m outwards, and is 5 m deep with three soil layers characterizing the unsaturated soil, with the 2.5-5 m depth interval representing the weathered low conductivity saprolite that can store water but is inaccessible to tree roots. The 10 cm radius of the tree trunk domain was chosen so that the domain volume is approximately equal to that of the sapwood of the real tree. Model solution also requires knowledge of the initial water potential distribution across the soil-tree domain. For the soil domain we converted the 24 soil moisture data of July 15 to soil water matric potential values using the laboratory-measured retention curves, and applied a 2nd order polynomial interpolation scheme to estimate the soil water potential across the measured soil domain, assuming hydraulic equilibrium at the domain boundaries.
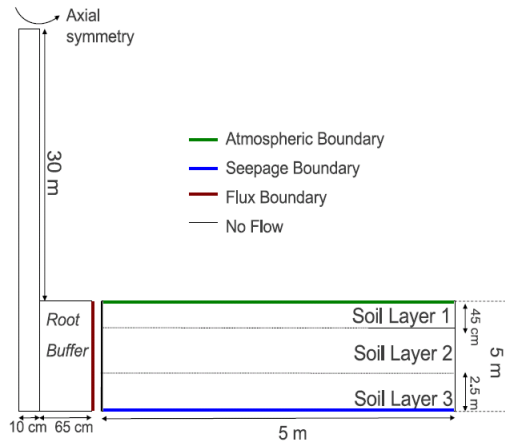
Fig. 1. Schematic of simulated SPAC domain.

Meteorological data from the weather tower were used to estimate local hourly potential evapotranspiration, ET_o , using the Penman-Monteith equation [29]. Values for the aerodynamic resistance and bulk surface stomatal resistance terms were calculated according to FAO guidelines (Allen et al., 1998). To estimate the potential tree transpiration, ET_p, we adopted the crop coefficient approach [30], and multiplied ET_o with a tree coefficient, s_{ETo} (-) , or

$$ET_p = s_{ETo}ET_o \tag{4}$$

Moreover, because of the soil dryness for the selected monitoring period, we could assume that soil evaporation was nil. The lower boundary of the soil at the 5 m depth was described by a seepage boundary, allowing water to leave the soil domain when saturated, and more importantly allowing for both upwards and downwards flow across the whole soil domain.

3.3. Coupling of root water uptake with tree canopy transpiration.

Root water uptake is simulated by the *W*-term in Eq. [1], representing actual uptake (m^3 m^{-3} day^{-1}) at each node in the soil domain, controlled by root density distribution, β_{Soil} *(r,z)* (m^{-3})*,* and a soil water stress response function, γ_{Soil} *(h)*. Both have functional values between 0 and 1. For an axisymmetrical soil domain Ω,, the normalized root water uptake distribution, β_{Soil} *(r,z)* is defined by [31,32]:

$$\beta_{soil}(r,z) = \frac{\beta^*}{2\pi \int_\Omega r\beta^* d\Omega} \tag{5a}$$

with a general nonuniform root distribution, β^*, as defined by [31]:

$$\beta^*(r,z) = \left[\left(1-\frac{z}{z_m}\right)\right]\left[\left(1-\frac{r}{r_m}\right)\right]e^{-\left(\frac{p_z}{z_m}|z^*-z|+\frac{p_r}{r_m}|r^*-r|\right)} \tag{5b}$$

where r_m and z_m define the maximum rooting extent in the radial and depth direction (m). z^* and r^* are empirical parameters (m) that shift the maximum of the distribution in vertical and radial direction,

respectively, and p_z and p_r are empirical parameters that determine the exponential shape of the distribution.

For water-stressed soil conditions, the actual root water uptake term in Eq. (1) is computed from:

$$W(h,r,z) = \gamma_{soil}(h)\beta_{soil}(r,z)\pi r_m^2 \, ET_p \qquad (6)$$

where $\gamma_{soil}(h)$ (dimensionless) was introduced by Feddes et al. [33], and reduces root water uptake from its maximum possible value because of soil water stress. The Feddes function is defined by four water potential values, P_1 through P_4. For soil water potential values between P_2 and P_3, $\gamma_{soil}(h)$ will be optimum and equal to 1.0. For h-values between P_1 and P_2 (soil aeration stress) and between P_3 and P_4 and lower (soil water stress), γ_{soil} values will be smaller than one and zero, at a minimum ($h < P_4$). Finally, from integration of Eq. (5) over the soil domain, the actual total root water uptake, R_a, (m d^{-1}) is computed from:

$$R_a = \frac{2\pi}{\pi r_m^2} \int_\Omega rW d\Omega \qquad (7)$$

In the presented coupled domain, the volume of water taken up by the roots must now be transported in the conducting vessels (xylem) of the sapwood in the tree trunk. For that purpose, the coupled model includes a small storage reservoir to simulate the root domain that temporally holds it, and empties it into the tree's sapwood domain by way of defining a lower flux boundary condition for the tree domain..

To simulate tree transpiration, we introduce a sink term, $W(h,z)$, which is a function of the one-dimensional canopy density distribution function, $\beta_{tree}(z)$, and a canopy water stress response function, $\gamma_{tree}(h)$. We define the canopy distribution (m^{-1}) by:

$$\beta_{tree}^*(z) = 1 - \left(\frac{z-6}{24}\right) \quad , , \qquad (8)$$

for $z > 6$ m and zero otherwise. After normalization, and defining a canopy stress function that is of a similar Feddes form as used for characterizing soil water stress, the actual tree transpiration (ET_a) is computed from:

$$ET_a = \frac{2\pi}{\pi r_m^2} \int_\Omega rW_{tree}(h,r,z)dz = 2\pi R_a \int_\Omega r\gamma_{tree}(h)\beta_{tree}(r,z) \, dz \qquad (9)$$

We realize that $R_a = ET_a$, only if the tree trunk water storage is not changing over the time period of the calculation. In all, this approach clearly shows the coupling of root water uptake with tree transpiration, by way of the stress response functions for root water uptake and canopy transpiration, which are defined by soil water potential and stem water potential, respectively.

4. Parameter optimization

The presented continuum model includes numerous parameters, of which we selected 18 of them to be unknown, apriori, to be estimated using the MT-DREAM optimization method [34]. Soil water retention and unsaturated hydraulic conductivity parameters of Eqs. [2] and [3] for the top two soil layers were partly determined from laboratory experiments (α and n), however, corresponding k_s and θ_s values for each layers were considered unknown parameters. We assumed the soil hydraulic parameter values for the third 2.5-5 m layer to be equal to those of the second layer, except the k_s value was reduced by two orders of magnitude. All tree hydraulic parameters (α_{tree}, n_{tree} , $k_{s,tree}$ and $\theta_{s,tree}$) were assumed unknown and were part of the optimized parameter set. The residual water content value ($\theta_{r,tree}$) was set to zero.

Maximum rooting extend in the vertical (z_m = 1.6 m) and lateral direction (r_m =5.0 m) were known from root excavation data for a similar nearby tree, but all other four parameters (z^*, r^*, p_z, and p_r) were optimized. Stress response function parameters, P_1 through P_4, were partially assumed known. For the soil water stress function we only optimized P$_3$, whereas other values were fixed to $P_{1,soil}$ = -1 kPa , $P_{2,soil}$ = -2.5 kPa, and $P_{4,soil}$ = -2,000 kPa. For the canopy water stress response function, both values of P_3 and P_4 were optimized, with fixed values of $P_{1,tree}$ = -1 kPa , $P_{2,tree}$ = -0.2 kPa. Finally, we introduced a sap flow scaling parameter, s_{sap}, to adjust the magnitude of measured sap flow rates to those required from measured soil water storage changes, or

$$q_{sap} = s_{sap} \ q_{sap, measured} \qquad\qquad (10)$$

as sap flow measurements are known to accurately represent tree sap flow dynamics, however, their magnitudes are typically uncertain.

We applied a global Markov Chain Monte Carlo (MCMC) optimization framework that allows for (a) large number of unknown parameters, (b) different measurement types, and (c) quantification of parameter uncertainty. Specifically, we used the DiffeRential Evolution Adaptive Metropolis (DREAM) family of algorithms [34,35,36,37]. To find the best possible agreement between a series of N observations Y = Y$_1$ . . . Y$_N$ and N simulated values y = y$_1$ . . . y$_N$, the parameter optimization technique minimizes the objective function, SS, that contains the sum of squares of residuals between simulated and measured variables, or

$$SS = \sum_{i=1}^{N} (y_i - Y_i)^2 \qquad\qquad (11)$$

This is accomplished through iterative solution of the hydrodynamic STAC model, changing parameters of the optimized parameter vector, ξ. MCMC methods guide Markov chains on a random walk through the parameters space. The final optimization result includes a posterior distribution of optimized values for each of the optimization vector, ξ, from which parameter uncertainty can be derived. The MT-DREAM algorithm optimizes the parameter in parallel through multiple chains of parameter sets, and it is therefore that the solution is most efficiently run on a computer cluster.

5. Results and Discussion

An important result of parameter optimization is the correlation between optimized parameters. That is, high parameter correlation is an indication of nonuniqueness between the correlated parameters, and likely will also present itself by a wide postiori and multimodel distribution of those parameters. We found strong correlation between the parameters α_{tree} and n_{tree} , as also determined by Huisman et al., [38] and between $k_{s,tree}$ and the sapflow scaling factor, s$_{sap}$. The final optimized tree water relationships are presented in Fig. 2a (tree water retention curve) and Fig. 2b(tree relative conductivity curve). The optimized curves using the median of the optimized parameter distributions are represented by the green solid lines, with the blue area characterizing the uncertainty as defined by the 95% confidence interval of the posterior distribution, as calculated by a bootstrapping technique.

The tree water retention curve agrees well with literature data [39, 40] The agreement with literature values for the relative hydraulic conductivity curve is not as good, but is especially very good when compared with the Waring and Running [39] experimental data for a white fir (orange crosses).However, in all honesty, we should not always expect agreement, as referenced experimental tree hydraulic data are typically collected from small tree branches or wood cuttings, whereas our tree water relationships represent effective hydraulic functions for the sapwood of the whole tree.
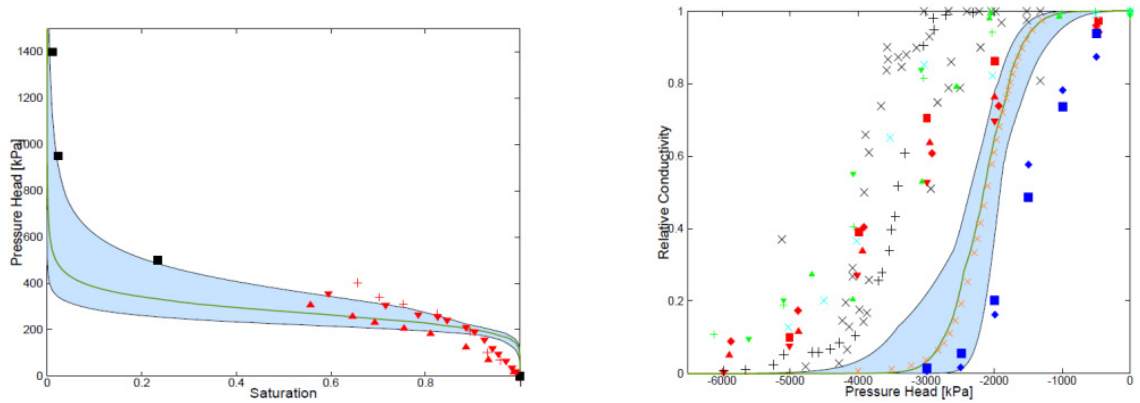
Fig. 2. Comparison of independently measured (symbols) with optimized tree water relationships, (a) tree water retention curve; (b) tree hydraulic conductivity functions

Comparison of measured and simulated hydrologic variables are presented in Fig. 3, for ET_p (cm/d), sap flux (L/h), stem water potential (kPa) and soil water storage (m^3) for the simulated 18-day period of July, 2009. The ET data in the top panel compares potential ET using the flux tower weather data (blue) with the scaled ET (ET_p) using the tree coefficient, s_{ETo}. Given the uncertainty of the data, the model fit is an excellent agreement with soil and tree observations.
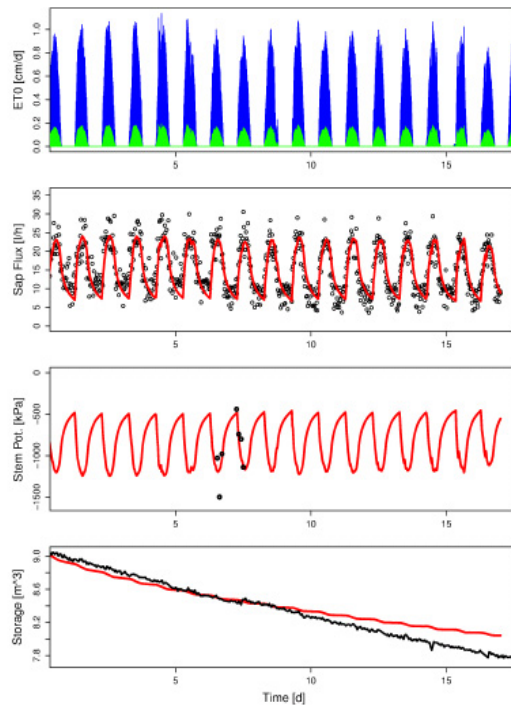

Fig. 3. Comparison of measured with simulated ETp, sap flow, stem water potential, and soil water storage

Figure 4 presents diurnal fluctuations in tree water potential (left panel) and sapflow (right panel) for a period of 48 hours during the 18-day simulation period, at 10 heights, from the base of the tree (1 m) to the top of the tree at 28 m.

As expected, diurnal fluctuations increase as one moves from the base to the top of the tree, as controlled by the reduced water delivery by sapflow upwards into the tree canopy. Canopy stress is mostly felt towards the top of the tree canopy, with stem water potential approaching -2,000 kPa. We note that the optimized $P_{3,tree}$ value was -1,500 kPa, indicating that the tree was under water stress during part of the day.

We also note the recovery of stem water potential overnight, as determined by the refilling of the water-conducting vessels (right panel, Fig. 4). As is intuitively clear, sapflow decreases from the tree base towards the top of the tree because of tree transpiration. The largest diurnal fluctuations in sap flow occur near the base of the tree with high sap flow values during the day, decreasing towards zero overnight, and refilling the water conducting sap wood in the tree trunk. The magnitude of the diurnal fluctuations is controlled by both atmospheric forcing and the tree water relationships. The tree water retention curve controls the water capacity of the tree and the temporal variations in tree water potential and sap water content, whereas the relative conductivity functions controls sap flow rate and water delivery to the transpiring canopy, as well as the rate of water redistribution, replenishing the decreasing water storage in the water-stressed sapwood and canopy.
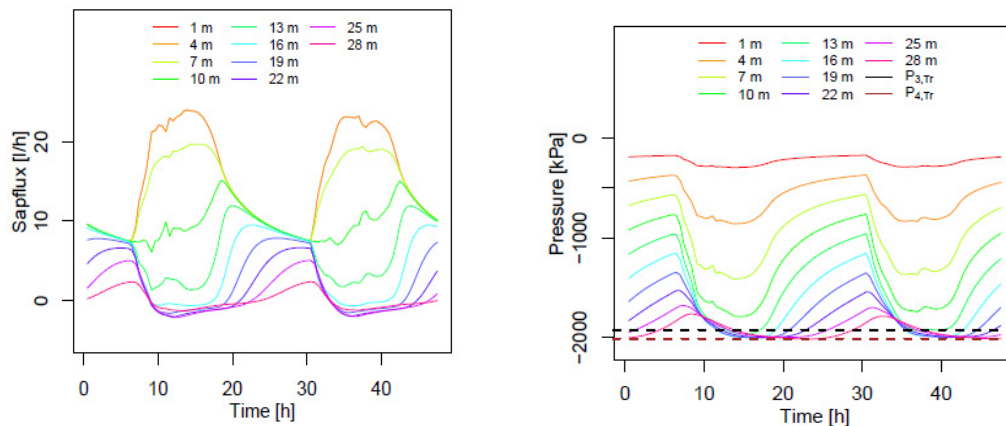

Fig. 4 Simulated sap flow (left panel) and corresponding stem water potential (right panel) for 10 tree heights for a 48-period

Acknowledgements

References

[1]Van der Honert TH.. Water transport in plants as a catenary process. *Discussions of the Faraday Society* 1948;**3**:146–153.
[2]Waring RH, Whitehead D, Jarvis PG. The contribution of stored water to transpiration in Scots pine. *Plant Cell Environ*. 1979;**8**:613-622.

[3]Jarvis PG, Edwards WRN, Talbot H. Models of crop water use. Academic Press, London, 1981; Vol.35.

[4]Cowan IR. Transport of water in the soil-plant-atmosphere system. *Journal of Applied Ecology* 1965;**2**:221–239.

[5]Tyree MT. A dynamic model water flow in a single tree: evidence that models must account for hydraulic architecture. *Tree Physiology* 1988;**4**:195–217.

[6]Da Silva D, Favreau R, Auzmendi I, De Jong, TM.. Linking water stress effects on carbon partitioning by introducing a xylem circuit into L-PEACH. *Annals of Botany* 2011.

[7]Aumann CA, Ford CE. Modeling tree water flow as an unsaturated flow through a porous medium. *Journal of Theoretical Biology* 2002;**219**:415–429.

[8]Frueh T, Kurth W.. The hydraulic system of trees: theoretical framework and numerical simulation. *Journal of theoretical Biology* 1999;**201**:251–270.

[9]Kumagai T. Modeling water transportation and storage in sapwood model development and validation. *Agricultural and Forest Meteorology* 2001;**109**:105–115.

10]Bohrer G, Mourad H, Laursen TA, Drewry D, Avissar R, Poggi D,Oren R, Katul GG. Finite element tree crown hydrodynamics model (FETCH) using porous media flow within branching elements: A new representation of tree hydrodynamics. *Water Resources Research* 2005;**41**, W11404.

[11]Chuang YL, Oren R, Bertozzi AL, Phillips N, Katul GG. The porous media model for the hydraulic system of a conifer tree: Linking sap flux data to transpiration rate. *Ecological Modelling* 2006;**191**:447–468.

[12]Janott M, Gayler S, Gessler A, Javaux M, Klier C, Priesack E. A one-dimensional model of water flow in soil-plant systems based on plant architecture. *Plant and Soil* 2011;**341**:233–256.

[13]Siqueira M, Katul G, Porpato A. Onset of water stress, hysteresis in plant conductance, and hydraulic lift: Scaling soil water dynamics from millimeters to meters. *Water Resour. Res*. 2008;**44**, W01432, doi:1029/2007WR006094.

[14]Simunek J, van Genuchten MT, ˇSejna M. Development and applications of the hydrus and stanmod software packages and related codes. *Vadose Zone Journal* 2008;**7**:587–600.

[[15]Bittner S, Legner N, Beese F, Priesack E. Individual tree branch-level simulation of light attenuation and water flow of three F. sylvatica L. trees. *J. Geophys. Res.* 2012;**117**, G01037,doi:10.1029/2011JG001780.

[16]Richards LA.. Capillary conduction of liquids through porous mediums. *Physics* 1931;**1**:318–333.

[17]Bittner S, Janott M, Ritter D, Kocher P, Beese F, Priesack E. Functional-structured water flow model reveals differences between diffuse and ring porous tree species. *Agric. And Forest Meteorology* 2012;**159-9**:80-89.

[18]Eching SO; Hopmans JW. . Optimization of hydraulic function from transient outflow and soil water pressure data. *Soil Sci. Soc. Amer. J.* 1993;**57**:1167-1175.

[19]Hopmans JW, Simunek J, Romano N, Durner W. Simultaneous determination of water transmission and retention properties. Inverse Methods. In: *Methods of Soil Analysis. Part 4. Physical Methods*. (J.H. Dane and G.C. Topp, Eds.). Soil Science Society of America Book Series N. 5, 2002; p.963-1008.

[20]Bales RC, Conklin MH, Kerkez B, Glaser S, Hopmans JW, Hunsaker CT, Meadows M, Hartsough PC. *Forest Hydrologyand Biogeochemistry: Synthesis of Past Research and Future Directions*. Springer Science+Business Media. chapter Sampling Strategies in ForestHydrology and Biogeochemistry, 2011a.

[21]Bales RC, Hopmans JW, O'Geen AT, Meadows M, Hartsough PC, Kirchner P, Hunsaker CT, Beaudette D. Soil moisture responseto snowmelt and rainfall in a Sierra Nevada mixed-conifer forest. *VadoseZone Journal* 2011b;**10**:786–799.

[22]Reynolds WD, Elrick DE. Saturated and field-saturated water flow parameters. In J.H. Dane, and G.C. Topp (ed.) *Methods of soil analysis: Part 4 -physical methods*. Soil Science Society of America, Madison, USA. 2002; p.804-808

[23]Nasta P, Huynh S, Hopmans JW. Simplified Multistep Outflow Method to Estimate Unsaturated Hydraulic Functions for Coarse-textured Soils. *Soil Sci. Soc. Amer. J.* 2011;**75(2)**: doi:10.2136/sssaj2010.0113.

[24]Kizito F, Campbell CS, Campbell GS, Cobos DR, Teare BL, Carter B, Hopmans JW. Frequency, electrical conductivity and temperature analysis of a low-cost capacitance soil moisture sensor. *Journal of Hydrology* 2008;**352**:367–378.

[25]Green SR, Clothier BE. Water use of kiwifruit vines and apple trees by the heat-pulse technique. Journal of Experimental Botany 1988;**39**:115–123.

[26]Shackel KA, Ahmadi H. Plant water status as an index of irrigation need in deciduous fruit trees. *HortTechn* 1997;**7**:23–29.

[27]van Genuchten MT. A closed-form equation for predicting the hydraulic conductivity of unsaturated soils. *Soil Science Society of America Journal* 1980;**44**:892–898.

[28]Mualem Y. A new model for predicting the hydraulic conductivity of unsaturated porous media. *Water Resources Research* 1976;**12**:513–522.

[29]Allen RG, Pereira LS, Raes D, Smith M. *Crop evapotranspiration - Guidelines for computing crop water requirements*. Technical Report 56. FAO - Irrigation and Drainage, 1998.

[30]Doorenbos J, Pruitt WO. *Guidelines for predicting crop water requirements*. FAO Irrigation and Drainage 24, 1977.

[31]Vrugt JA, Hopmans JW, Šimunek J. Calibration of a two-dimensional root water uptake model. *Soil Sci. Soc. Am. J.* 2001a;**65**:1027–1037.

[32]Gardenas A, Hopmans JW, Hanson BR, Šimunek J. Two-dimensional modeling of Nitrate Leaching for Different Fertigation Strategies under Micro-Irrigation. Agric. *Water Management* 2005;**74**:219-242.

[33]Feddes RA, Kowalik PJ, Zaradny H. *Simulation of Field Water Use and Crop Yield*. John Wiley & Sons, Inc., NY. 1978.

[34]Vrugt JA, Laloy E, ter Braak CJF, Hyman JM. Posterior exploration using differential evolution adaptive Metropolis with sampling from past states. 2011, in preparation.

[35] Vrugt JA, ter Braak CJF, Clark MP, Hyman JM, Robinson BA. Treatment of input uncertainty in hydrologic modeling: Doing hydrology backward with Markov chain Monte Carlo simulation. *Water Resources Research* 2008;**44**, W00B09.

[36] Vrugt JA, ter Braak CJF, Diks CGH, Robinson BA, Hyman JM, Higdon D. Accelerating Markov Chain Monte Carlo simulations by differential evolution with self-adaptive randomized subspace sampling. *International Journal of Nonlinear Sciences and Numerical Simulation* 2009;**10**:273–290.

[37]Laloy E, Vrugt JA. High-dimensional posterior exploration of hydrologic models using multiple-try DREAM(ZS) and high performance computing. *Water Resources Research* 2012; doi:10.1029/2011WR010608.

[38]Huisman JA, Rings J, Vrugt JA, Sorg J, Vereecken H. Hydraulic properties of a model dike from coupled Bayesian and multi-criteria hydrogeophysical inversion. *Journal of Hydrology* 2010;**380**:62–73.

[39] Waring RH, Running SW. Sapwood water storage: its contribution to transpiration and effect upon water conductance through the stems of old-growth Douglas-fir. *Plant, Cell and Environment* 1978;**1**:131–140.

[40] Yoder BJ. *Comparative Water Relations of Abies grandis, Abies concolor and their hybrids*. Master's thesis. Oregon State University, 1984.